

# Inertia-aware Unit Commitment and Remuneration Methods for Decarbonized Power System

Hyun Joong Kim, *Member, IEEE*, and Jip Kim, *Member, IEEE*,

**Abstract**—To maintain frequency stability in decarbonized power systems, inertia services from synchronous generators (SGs) and inverter-based resources must be procured. However, designing an inertia-aware system operation poses significant challenges in considering the variability and uncertainty of renewable energy sources (RES) and adopting a remuneration method for inertia provision due to SG commitment variables. To address this research gap, we renovate the inertia-aware chance constraints unit commitment model by incorporating time-coupling constraints for SGs and joint chance constraints for RES uncertainty. We investigate remuneration methods for inertia provision, including uplift, marginal pricing (MP), approximated convex hull pricing (aCHP), and average incremental cost pricing (AIP), applying these to the renovated model. Numerical experiments show that the model enhances frequency stability during a contingency. Among the remuneration methods, only aCHP guarantees revenue adequacy without requiring uplift while maximizing economic welfare. However, the MP requires the highest level of uplift to adequately compensate generation costs, as the price function fails to account for inertia provision.

**Index Terms**—Inertia-aware operation, unit commitment, remuneration methods, power grid decarbonization

## I. INTRODUCTION

OVER the past decades, the penetration of renewable energy sources (RES) has rapidly increased following a global paradigm shift toward decarbonization. According to [1], the capacity of the photovoltaic generator (PV) and wind turbine (WT) have increased from 40 GW and 181 GW in 2010 to 1,055 GW and 899 GW in 2022. However, this rapid penetration of RES leads to a consequential reduction in the rotational inertia provided by synchronous generators (SG), raising concerns regarding frequency stability.

One potential solution is to harness the capabilities of inverter-based resources (IBRs) to deliver fast frequency response (FFR) [2]–[4]. According to [5], FFR can be provided by various control mechanisms that inject additional power before the frequency nadir is reached after a sudden power imbalance. Sustained FFR can maintain the change in power injection until secondary frequency controls return the system to the nominal frequency. It is coordinated with the primary frequency response to arrest the frequency nadir and support the recovery of the nominal frequency. In contrast, only the inertial response, unsustained FFR, can decelerate the rate of change of frequency (RoCoF) by transferring stored kinetic

energy from SGs to power injection or using control actions of IBRs that mimic this behavior [6].

A significant reduction in system inertia can result in a very high RoCoF [7]. Elevated RoCoF reflects a rapid frequency decline during contingency events, potentially disrupting under-frequency load shedding mechanisms, which rely on early-stage frequency detection and response. Such disruptions may lead to blackouts or frequency collapse. Additionally, reduced inertia impairs the ability of the system to damp oscillations [8], and therefore, maintaining RoCoF within acceptable limits by ensuring sufficient inertia is critical for preserving frequency stability.

Independent system operators (ISO) are actively working to secure system inertia. The Electric Reliability Council of Texas (ERCOT) addresses inertia shortages by deploying reliability must-run (RMR) units when system inertia drops below 105 GW-s [9], [10]. To minimize market disruptions, RMR units operate at a minimum generation level [11]. However, these units typically have high marginal costs, making it difficult to achieve revenue adequacy through market energy prices alone. To address this, ERCOT contracts RMR units and compensates eligible costs [12]. Similarly, the transmission system operator (TSO) Eirgrid mandates a minimum system inertia of 23 GW-s [13]. While this requirement ensures frequency stability, interventions in system operation—deviating from economic dispatch principles—raise overall generation costs. To ensure revenue adequacy for inertia providers, Eirgrid currently employs regulated tariffs but plans to transition to an inertia market [13]. The Australian Energy Market Commission (AEMC) also tackles inertia scarcity, promoting virtual inertia through market mechanisms [14] and intervening directly to commit sufficient SGs during inertia shortfalls [15]. However, AEMC faces challenges in creating the inertia market because inertia is discretely determined by the commitment of SGs.

Several studies have explored strategies to ensure adequate inertia and quantify the value of inertia contributions to the power system. For instance, the authors in [16], [17] have proposed an inertia market that operates based on bids from service providers, and suggested a methodology for a frequency-constrained unit commitment (UC) model. However, these approaches neglect the stochastic nature of RES, particularly under high RES penetration. To address this limitation, the authors in [18]–[20] propose chance-constrained methods for designing electricity markets considering inertia services and requirements. Nevertheless, these studies fail to account for time-coupling constraints, such as ramping and minimum up/down time constraints, which can affect the commitment of SGs. Moreover, they overlook joint chance constraints that

The authors are with the Institute for Grid Modernization, Department of Energy Engineering, KENTECH, Republic of Korea. This work was supported by National Research Foundation of Korea (NRF) grant funded by the Korean government (MIST) (No. RS-2023-00210018) and KENTECH Research Grant (202300008A).

consider the uncertainties associated with heterogeneous RES.

While [16]–[20] incorporate inertia services into market clearing mechanisms, they have focused on methodologies for inertia pricing and have not provided in-depth analysis comparing other pricing methods, which are essential when determining remuneration methods for inertia provision. Moreover, when employing an UC-based model, the inertia price derived from the dual variables of inertia requirement can be zero value. Uplift is also considered as a means to ensure revenue adequacy for inertia providers [21]. However, uplift mechanisms have notable drawbacks, including the failure to provide effective market price signals for system planning and operation, ultimately disrupting the economic equilibrium of the market. To overcome this limitation, a method for deriving inertia prices using convex hull pricing, which forcibly formulates an inertia price by relaxing the non-convexity through the commitment variables of SG, has been proposed [22], [23]. Additionally, the average incremental pricing method, which can derive inertia price by converting non-load and start-up costs into average incremental costs based on UC results and relaxing commitment variables, can be an alternative approach to determine the value of inertia [24]. Despite these advancements, existing studies still lack comprehensive insights into developing robust remuneration methods for inertia provision.

In this context, we enhance a chance-constrained inertia-aware UC model that co-optimizes energy, reserves, and inertia provision in a decarbonized power system. Additionally, we investigate three remuneration methods for inertia provision based on the results of the chance-constrained inertia-aware UC. The key contributions of this work are as follows:

- 1) Building on [18], [20], we refine the model by incorporating the ramping and minimum up/down time constraints of SGs and joint chance constraints of uncertainty of PV and WT. Consequently, the model can utilize PV, WT, energy storage (ES), and SG to secure sufficient inertia.
- 2) We investigate remuneration methods such as uplift, marginal pricing (MP), approximated convex hull pricing (aCHP), and average incremental pricing (AIP). Uplift makes up for the economic losses, which cannot be compensated by market prices, for additional generation costs associated with inertia provision; MP derives the energy, reserve, and inertia price through the dual variables in the chance-constrained UC (CC-UC) and ED problem; aCHP separates the multi-hour pricing problem into individual single-hour pricing problems by distributing commitment costs across a series of operational hours [25]. AIP calculates prices through the same process as aCHP but converts non-load and start-up costs into average variable costs.
- 3) We demonstrate that our renovated inertia-aware operation can enhance the frequency stability following a contingency. We compare the remuneration methods according to the inertia-aware system operation. Based on the simulation results, aCHP minimizes an uplift and ensures revenue adequacy for individual generators; however, MP, and AIP cannot ensure revenue adequacy for individual generators without an uplift. MP fails to

provide a price signal for inertia provision.

## II. PRELIMINARIES

This section introduces uncertainty generation and inertia provision models for RES and joint chance constraints. More details can be found in [20].

### A. Uncertainty of generation

Denoting  $\mathbf{P}_{pi,t}$  as a random variable for PV, which are consisting the generation forecast  $P_{pi,t}$  and the forecast error  $\omega_{pi,t}$ . Similarly, a random variable for WT  $\mathbf{P}_{wi,t}$  can be defined using  $P_{wi,t}$  and  $\omega_{wi,t}$ . The uncertainty of renewable power can be modeled as follows [20]:

$$\mathbf{P}_{pi,t} = P_{pi,t} - \omega_{pi,t}, \quad (1a)$$

$$\mathbf{P}_{wi,t} = P_{wi,t} - \omega_{wi,t}. \quad (1b)$$

It is assumed that  $\omega_{pi,t}$  and  $\omega_{wi,t}$  follow a normal distribution of forecast errors, i.e.,  $\omega_{pi,t} \sim \mathcal{N}(m_{pi,t}, \sigma_{pi,t}^2)$  and  $\omega_{wi,t} \sim \mathcal{N}(m_{wi,t}, \sigma_{wi,t}^2)$ , where  $m_{pi,t}$  and  $m_{wi,t}$  represent the mean of normal distributions and  $\sigma_{pi,t}^2$  and  $\sigma_{wi,t}^2$  denote the variance of forecast errors for PV and WT generation across time  $t$  and node  $i$  [26]. Although the power generation of RES is influenced by climate, forecast errors vary depending on the forecasting methods and tools. Assuming the forecast errors for PV and WT generation are mutually independent [27], the system-wide uncertainty resulting from forecast errors  $\omega_{pi,t}$  and  $\omega_{wi,t}$  can be defined as:

$$\Omega_{rt} = \sum_{i \in \mathcal{I}} \omega_{pi,t} + \omega_{wi,t}, \quad (2)$$

which follows a normal distribution, i.e.,  $\Omega_{rt} \sim \mathcal{N}(M_{rt}, \Sigma_{rt}^2)$ , where  $M_{rt} = \sum_{i \in \mathcal{I}} m_{pi,t} + m_{wi,t}$ , and  $\Sigma_{rt}^2 = \sum_{i \in \mathcal{I}} \sigma_{pi,t}^2 + \sum_{i \in \mathcal{I}} \sigma_{wi,t}^2$ .

### B. Uncertainty of inertia provision

Since the inertia provision of PV and WT at node  $i$  depends on uncertain atmospheric phenomena, the inertia by PV and WT are also random and time-varying variables as follows:

$$\mathbf{H}_{pi,t} = H_{pi,t} - \omega_{phi,t}, \quad (3a)$$

$$\mathbf{H}_{wi,t} = H_{wi,t} - \omega_{whi,t}, \quad (3b)$$

where,  $\omega_{phi,t}$  follows a normal distribution with mean  $m_{phi,t}$  and  $m_{whi,t}$  and the variance of forecast errors  $\sigma_{phi,t}^2$  across time  $t$  and node  $i$ . Similarly,  $\omega_{whi,t}$  also follows a normal distribution with mean  $m_{whi,t}$  and the variance and the variance of forecast errors  $\sigma_{whi,t}^2$ , i.e.,  $\omega_{phi,t} \sim \mathcal{N}(m_{phi,t}, \sigma_{phi,t}^2)$  and  $\omega_{whi,t} \sim \mathcal{N}(m_{whi,t}, \sigma_{whi,t}^2)$ . Furthermore, system-wide inertia forecast error of RES can be defined by:

$$\Omega_{ht} = \sum_{i \in \mathcal{I}} \omega_{phi,t} + \omega_{whi,t}, \quad (4)$$

where  $\Omega_{ht}$  also follows a normal distribution with mean  $M_{ht} = \sum_{i \in \mathcal{I}} m_{phi,t} + m_{whi,t}$  and  $\Sigma_{ht}^2 = \sum_{i \in \mathcal{I}} \sigma_{phi,t}^2 + \sum_{i \in \mathcal{I}} \sigma_{whi,t}^2$  denotes the variance of forecast errors. Note that both wind power and inertia forecast errors,  $\omega_{wi,t}$  and  $\omega_{whi,t}$ , are influenced by wind speed. However, the inertia

control technique for PV is based on generation deloading [28]. The deloading technique ensures a reserve margin by shifting the operating point of PV from its optimal power extraction curve to a reduced power level. Assuming that PV performs deloading operations and provides inertia through a reserve margin sufficient to remain unaffected by changes in atmospheric phenomena, the inertia of PV is mutually independent of PV generation and the inertia provided by WT. Furthermore,  $\omega_{whi,t}$  and  $\omega_{wi,t}$  are not included in the same chance constraint within the renovated model. The deterministic equivalent formulation only requires each random variable to be represented by a normal distribution without making any assumptions about its dependency [20].

### III. INERTIA-AWARE CHANCE CONSTRAINED UNIT COMMITMENT

This section renovates an inertia-aware CC-UC model for the RES-dominant power system. System operations employ stochastic optimization methods to address the joint chance constraints of the uncertainty of RES and time coupling constraints of SG. This framework enables resources to contribute to enhancing system reliability.

The market model in (5) represents the inertia-aware chance-constrained UC, including SG, ES, PV, and WT.

$$\min_{\Xi} \sum_{t \in \mathcal{T}} \sum_{i \in \mathcal{I}} \mathbb{E}_{\Omega_{rt}} [c_{gi}(\mathbf{P}_{gi,t}, u_{gi,t}, v_{gi,t})] \quad (5a)$$

$$\text{s.t. } \forall i \in \mathcal{I}, \forall t \in \mathcal{T}:$$

$$u_{gi,t}, v_{gi,t}, w_{gi,t} \in \{0, 1\}, \quad (5b)$$

$$u_{gi,t} - u_{gi,t-1} = v_{gi,t} - w_{gi,t}, \quad \forall t \in [2, T], \quad (5c)$$

$$\sum_{\tau=t-TU_{gi}+1}^t v_{gi,\tau} \leq u_{gi,t}, \quad \forall t \in [TU_{gi}, T], \quad (5d)$$

$$\sum_{\tau=t-TD_{gi}+1}^t w_{gi,\tau} \leq 1 - u_{gi,t}, \quad \forall t \in [TD_{gi}, T], \quad (5e)$$

$$-RD_{gi} \leq p_{gi,t} - p_{gi,t-1} \leq RU_{gi}, \quad (5f)$$

$$0 \leq \alpha_{gi,t} \leq u_{gi,t}, \quad (5g)$$

$$\mathbb{P}_{\Omega_{rt}}[\mathbf{P}_{gi,t} \leq u_{gi,t} P_{gi}^{\max}] \geq 1 - \epsilon_{gi}, \quad (5h)$$

$$\mathbb{P}_{\Omega_{rt}}[\mathbf{P}_{gi,t} \geq u_{gi,t} P_{gi}^{\min}] \geq 1 - \epsilon_{gi}, \quad (5i)$$

$$\mathbb{P}_{\Omega_{rt}}[\mathbf{P}_{di,t} + 2H_{ei,t} f'_{\max} P_{ei}^{\max} / f_0 \leq P_{ei}^{\max}] \geq 1 - \epsilon_{di}, \quad (5j)$$

$$\mathbb{P}_{\Omega_{rt}}[\mathbf{P}_{ci,t} + 2H_{ei,t} f'_{\max} P_{ei}^{\max} / f_0 \leq P_{ci}^{\max}] \geq 1 - \epsilon_{ci}, \quad (5k)$$

$$e_{i,t} \leq E_i^{\max} - 2H_{ei,t} \Delta f_{\max} P_{ei}^{\max} / f_0, \quad (5l)$$

$$e_{i,t} \geq E_i^{\min} + 2H_{ei,t} \Delta f_{\max} P_{ei}^{\max} / f_0, \quad (5m)$$

$$e_{i,t} = e_{i,t-1} + \mathbb{E}_{\Omega_{rt}}[\mathbf{P}_{ci,t} k_i - \mathbf{P}_{di,t} / k_i], \quad (5n)$$

$$0 \leq \alpha_{ci,t}, \alpha_{di,t} \leq 1, \quad (5o)$$

$$H_{ei,t} \leq H_{ei}^{\max}, \quad (5p)$$

$$-F_{i,j}^{\max} \leq B_{i,j}(\theta_{i,t} - \theta_{j,t}) \leq F_{i,j}^{\max}, \quad (5q)$$

$$\begin{aligned} & P_{gi,t} + P_{di,t} - P_{ci,t} + P_{wi,t} + P_{pi,t} - D_{i,t} \\ &= \sum_{j \in \mathcal{N}_i} B_{i,j}(\theta_{i,t} - \theta_{j,t}), \end{aligned} \quad (5r)$$

$$\sum_{i \in \mathcal{I}} (\alpha_{gi,t} + \alpha_{di,t} - \alpha_{ci,t}) = 1, \quad (5s)$$

$$\begin{aligned} & \mathbb{P}_{\Omega_{ht}} \left[ \sum_{i \in \mathcal{I}} (u_{gi,t} H_{gi} P_{gi}^{\max} + H_{ei,t} P_{ei}^{\max} \right. \\ & \left. + H_{pi,t} P_{pi}^{\max} + H_{wi,t} P_{wi}^{\max}) \geq P_{sys} H_{\min} \right] \geq 1 - \epsilon_{hi}, \end{aligned} \quad (5t)$$

where  $\Xi = \{p_{gi,t}, u_{gi,t}, v_{gi,t}, w_{gi,t}, \alpha_{gi,t}, p_{di,t}, p_{ci,t}, \alpha_{di,t}, \alpha_{ci,t}, H_{ei,t}\}$  being the set of optimization variables. Objective (5a) aims to minimize the total expected generation cost  $c_{gi}(\cdot)$  of the SG. Equations (5c) and (5e) ensure compliance with minimum up/down time constraints, where the status of the SG is indicated as on if  $u_{gi,t} = 1$  and off if  $u_{gi,t} = 0$ .  $v_{gi,t}$  and  $w_{gi,t}$  denote startup and shutdown status of SG, while  $TU_{gi}$  and  $TD_{gi}$  denote the minimum up/down time parameters for the SG. Ramping constraints are delineated in (5f). Given the variability of RES, the minimum up/down time and ramping constraints need to be incorporated into the model to ensure the reliable operation of the SGs. In (5g), the reserve participation factor for the SG is bounded between 0 and  $u_{gi,t}$ , implying that the SG cannot provide reserves when it is off. Chance constraints, as outlined in (5h) and (5i), represent the probability that the power output of the SG  $\mathbf{P}_{gi,t}$  remains within the maximum and minimum limits  $P_{gi}^{\min}$  and  $P_{gi}^{\max}$ . This probability should exceed  $1 - \epsilon_{gi}$ , where the risk level  $\epsilon_{gi} > 0$  is sufficiently small to be considered the violation of constraints of the SG acceptable. Chance constraints in (5j) and (5k) are used to guarantee an inertial response capable of addressing the maximum permissible RoCof  $f'_{\max}$  by limiting the ES charging and discharging power. Similarly, constraints (5l) and (5m) ensure a sufficient safety energy margin given by the maximum permissible frequency deviation at the frequency nadir  $\Delta f_{\max}$ . In (5n), the energy level of the ES is determined by considering the expected charging and discharging power with the normal distribution of forecast error. Constraints (5o)-(5p) limit charging and discharging power of ES, reserve participation factors of charging and discharging mode, and inertia constant of ES. Equations (5q) and (5r) are DC power flow constraints for the line thermal limits, which yields locational marginal prices when line congestion occurs. The constraint in (5s) maintains inertia provision by SG, ES, and RES with a probability of forecast error.

#### A. Deterministic Reformulation of Inertia-aware CC-UC

This section reformulates the expectation ( $\mathbb{E}$ ) and probability ( $\mathbb{P}$ ) operators into a tractable form for the model in (5).

1) *Reformulation of Expected Generation Cost:* Using the quadratic approximation, the generation cost of the SG is captured as:

$$\begin{aligned} & c_{gi}(\mathbf{P}_{gi,t}, u_{gi,t}, v_{gi,t}) \\ &= a_{gi}(\mathbf{P}_{gi,t})^2 + b_{gi} \mathbf{P}_{gi,t} + u_{gi,t} c_{gi} + v_{gi,t} s_{gi}, \end{aligned} \quad (6)$$

where  $a_{gi}$ ,  $b_{gi}$ ,  $c_{gi}$  are cost coefficients, and  $s_{gi}$  is start-up cost. Recalling that  $\mathbb{E}[\mathbf{x}^2] = \mathbb{E}[\mathbf{x}]^2 + \text{Var}[\mathbf{x}]$ , the expected generation cost in (6) is reformulated as follows:

$$\begin{aligned} & C_{gi,t} = \mathbb{E}_{\Omega_{rt}} [c_{gi}(\mathbf{P}_{gi,t}, u_{gi,t}, v_{gi,t})] \\ &= a_{gi} [(P_{gi,t} + M_{pt} \alpha_{gi,t})^2 + \Sigma_{pt}^2 \alpha_{gi,t}^2] \\ &+ b_{gi} (P_{gi,t} + M_{pt} \alpha_{gi,t}) + u_{gi,t} c_{gi} + v_{gi,t} s_{gi}. \end{aligned} \quad (7)$$

2) *Reformulation of Chance Constraints*: Assuming the random variables follow a normal distribution and have the inverse cumulative distribution function  $\Phi^{-1}(\cdot)$ , chance constraints can be transformed into deterministic forms [26]. To achieve deterministic formulation of (5), the following auxiliary parameters are defined:  $\hat{\delta}_{gi} = \Phi^{-1}(1 - \epsilon_{gi})\Sigma_{rt} - M_{rt}$ ,  $\hat{\delta}_{di} = \Phi^{-1}(1 - \epsilon_{di})\Sigma_{rt} - M_{rt}$ ,  $\hat{\delta}_{ci} = \Phi^{-1}(1 - \epsilon_{ci})\Sigma_{rt} - M_{rt}$ ,  $\hat{\delta}_{hi} = \Phi^{-1}(1 - \epsilon_{hi})\Sigma_{ht} - M_{ht}$ . Using the parameters, chance constraints such as, (5h), (5i), (5j), (5k), and (5t) are transformed into (8b)–(8g).

### B. Deterministic Equivalent of Inertia-aware CC-UC

Following the reformulation of expected generation cost and chance constraints, the deterministic equivalent of inertia-aware CC-UC is defined as:

$$\begin{aligned} \min \quad & \sum_{t \in \mathcal{T}} \sum_{i \in \mathcal{I}} C_{gi,t} \quad (8a) \\ \text{s.t.} \quad & (5b)–(5g), (5l)–(5s), \\ & P_{gi,t} \leq u_{gi,t} P_{gi}^{\max} - \hat{\delta}_{gi} \alpha_{gi,t}, \quad (8b) \\ & -P_{gi,t} \leq -u_{gi,t} P_{gi}^{\min} - \hat{\delta}_{gi} \alpha_{gi,t}, \quad (8c) \\ & P_{di,t} + 2H_{ei,t} f'_{\max} P_{ei}^{\max} / f_0 \leq P_{ei}^{\max} - \hat{\delta}_{di} \alpha_{di,t}, \quad (8d) \\ & P_{ci,t} + 2H_{ei,t} f'_{\max} P_{ei}^{\max} / f_0 \leq P_{ci}^{\max} - \hat{\delta}_{ci} \alpha_{ci,t}, \quad (8e) \\ & e_{i,t} = e_{i,t-1} + (P_{ci,t} + M_{pt} \alpha_{ci,t}) k_i \\ & \quad - (P_{di,t} + M_{pt} \alpha_{di,t}) / k_i, \quad (8f) \\ & \sum_{i \in \mathcal{I}} \left( u_{gi,t} H_{gi} P_{gi}^{\max} + H_{ei,t} P_{ei}^{\max} + (H_{pi,t} + \hat{\delta}_{hi}) P_{pi}^{\max} \right. \\ & \quad \left. + (H_{wi,t} + \hat{\delta}_{hi}) P_{wi}^{\max} \right) \geq P_{sys} H_{\min}. \quad (8g) \end{aligned}$$

The complete formulation can be found in Appendix A.

## IV. REMUNERATION METHODS FOR INERTIA-AWARE SYSTEM OPERATION

This section conceptualizes the remuneration methods (Uplift, MP, and aCHP) for securing the system inertia.

### A. Uplift

As a compensating method for RMR operation, we consider compensation cost, which covers the generation cost to provide system inertia. Meanwhile, IBRs that provide synthetic inertia using the deloading technique incur an economic loss in the market equivalent to the deloaded energy. Therefore, the uplift for RMR units and IBRs are defined as follows:

$$\Psi_{gi} = \sum_{t \in \mathcal{T}} (c_{gi}(p_{gi,t}) - \Lambda_t p_{gi,t}), \quad (9a)$$

$$\Pi_{gi} = \sum_{t \in \mathcal{T}} \Lambda_t (p_{gi,t}^{\text{mpppt}} - p_{gi,t}^{\text{del}}), \quad (9b)$$

where  $\Psi_{gi}$  is the compensation for the economic loss incurred by the settlement based on the market price  $\Lambda_t$ ,  $p_{ri,t}^{\text{mpppt}}$  denotes the maximum power output of the IBR at time  $t$ , and  $p_{gi,t}^{\text{mkt}}$  indicates the deloaded power output.

### B. Marginal pricing

Equation (8) is a mixed-integer quadratic program (MIQP), which can be solved using off-the-shelf solvers (e.g., CPLEX, Gurobi). After solving (5) and fixing the commitment variables  $u_{gi,t} = u_{gi,t}^*$ , an equivalent convex quadratic program (QP) can be defined as follows:

$$\min \quad \sum_{t \in \mathcal{T}} \sum_{i \in \mathcal{I}} C_{gi,t} \quad (10a)$$

$$\text{s.t.} \quad (5b)–(5g), (5l)–(5s), (8b)–(8g), \quad (10b)$$

$$u_{gi,t} = u_{gi,t}^*. \quad (10c)$$

Following [20], we derive marginal prices from dual variables of (10), which are the market price. Energy, reserve, and inertia prices are formulated below.

1) *Energy price in MP*: Energy price, which is the dual variable  $\lambda_{i,t}$  of (5r), is calculated based on the Karush-Kuhn-Tucker (KKT) optimality conditions as:

$$\begin{aligned} \lambda_{i,t} = & 2a_{gi}(P_{gi,t} + M_{pt} \alpha_{gi,t}) + b_{gi} \\ & + \mu_{i,t}^+ - \mu_{i,t}^- + v_{gi,t}^+ - v_{gi,t}^-, \quad (11) \end{aligned}$$

where  $\mu_{i,t}^+$  and  $\mu_{i,t}^-$  represent the dual variables associated with (5h) and (5j),  $v_{gi,t}^+$  and  $v_{gi,t}^-$  denote the dual variables related to (5f). Thus, energy price in MP is influenced by  $a_{gi}$  and  $b_{gi}$ .

2) *Reserve price in MP*: Reserve price, the dual variable  $\gamma_t$  of (5s), is defined as:

$$\begin{aligned} \gamma_t = & \frac{\sum_{i \in \mathcal{I}} [b_{gi} M_{pt} + (\mu_{i,t}^+ + \mu_{i,t}^-) \hat{\delta}_{gi} + \rho_{gi,t}^+ - \rho_{gi,t}^-] / 2a_{gi}}{\sum_{i \in \mathcal{I}} 1 / (2a_{gi})} \\ & + \frac{M_{pt} P_{gi,t} + [1 - \sum_{i \in \mathcal{I}} (\alpha_{di,t} - \alpha_{ci,t})] (\Sigma_{pt}^2 + M_{pt}^2)}{\sum_{i \in \mathcal{I}} 1 / (2a_{gi})}, \quad (12) \end{aligned}$$

where  $\rho_{gi,t}^+$  and  $\rho_{gi,t}^-$  represent the dual variables associated with (5g). It is noted that the reserve price, similar to the energy price, is also influenced by  $a_{gi}$  and  $b_{gi}$ .

3) *Inertia price in MP*: Based on the dual variables  $\chi_t$  of (5t), The inertia price can be formulated as follows:

$$\begin{aligned} \chi_t = & \frac{\sum_{i \in \mathcal{I}} [u_{gi,t} (c_{gi} - \mu_{i,t}^+ + \mu_{i,t}^- + \kappa_{i,t} - \rho_{i,t}^+)]}{P_{sys} H_{\min} - \sum_{i \in \mathcal{I}} [H_{ei,t} P_{ei}^{\max} + (H_{pi,t} + \hat{\delta}_{pi}) P_{pi}^{\max} + (H_{wi,t} + \hat{\delta}_{wi}) P_{wi}^{\max}]}, \quad (13) \end{aligned}$$

where  $\kappa_{i,t}$  represents the dual variable associated with (10c). If constraint (8g) is binding, while constraints (5h) and (5i) remain non-binding, the inertia price has a value. This value is affected by the non-load cost  $c_{gi}$  and the dual variable  $\kappa_{i,t}$  of the committed SG and increases as the inertia provided by the generator decreases. However, start-up costs do not affect the inertia price.

### C. Approximated convex hull pricing

This section introduces aCHP method for inertia-aware electricity markets. This method is a post-process aimed at determining the price, separate from operations [25].

1) *Convexified single-hour cost function*: To capture start-up cost into the prices, the generation cost defined in (7) is reformulated with the distributed start-up cost  $\tilde{s}_{gi,t}$  as:

$$\begin{aligned} \tilde{C}_{gi,t} = & a_{gi} [(P_{gi,t} + M_{pt}\alpha_{gi,t})^2 + \sum_{pt}^2 \alpha_{gi,t}^2] \\ & + b_{gi} (P_{gi,t} + M_{pt}\alpha_{gi,t}) + u_{gi,t}(c_{gi} + \tilde{s}_{gi,t}), \end{aligned} \quad (14)$$

where the start-up cost  $s_{gi}$  is allocated to online time  $t$  for the committed generators, which are decided in (8), i.e., the distributed start-up cost  $\tilde{s}_{gi,t}$  is represented as:

$$s_{gi} = \sum_t \tilde{s}_{gi,t}, \quad t \in [t_{on}, t_{off}]. \quad (15)$$

The reformulated generation cost  $\tilde{C}_{gi,t}$  is convexified by relaxing a commitment variable satisfying (8b), (8c) and:

$$0 \leq u_{gi,t} \leq 1, \quad \forall t \in \mathcal{T}, \forall i \in \mathcal{I}. \quad (16)$$

There are various guidelines for allocating the start-up cost of a generator during online time, and the market prices vary depending on the selection of the methods [25].

2) *Time decoupled convex equivalent*: The convex hull-based price at time  $t$  is obtained by minimizing the sum of the convexified single-hour cost of generator  $i$  as:

$$\min_{\Xi} \sum_{i \in \mathcal{I}} \tilde{C}_{gi,t} \quad (17a)$$

$$\text{s.t.} \quad (5f), (5g), (5q) - (5t), (8b), (8c), (8g), (16), \quad (17b)$$

where  $\Xi := \{p_{gi,t}, u_{gi,t}, \alpha_{gi,t}\}$  being the set of optimization variables. To calculate prices for operation hours, (17) must be solved for each time interval. In this process, the generation level at the previous time  $p_{gi,t-1}$  is fixed by the value determined by solving (17) for ramping constraints (5f). Furthermore, we assume the charging and discharging power, energy level, and hourly provided inertia of the ES are fixed based on the values determined from (8) because the charging and discharging power of an ES must be determined by the energy levels throughout the entire operational period.

3) *Energy price in aCHP*: By taking the partial derivative of the Lagrangian dual of (17) with respect to  $P_{gi,t}$ , energy price  $\lambda_{i,t}$  is derived as follow:

$$\begin{aligned} \lambda_{i,t} = & 2a_{gi}(P_{gi,t} + M_{pt}\alpha_{gi,t}) + b_{gi} \\ & + \mu_{gi,t}^+ - \mu_{gi,t}^- + v_{gi,t}^+ - v_{gi,t}^-. \end{aligned} \quad (18)$$

Equation (18) is identical to (11). This similarity shows that the variable generation cost of SG,  $a_{gi}$  and  $b_{gi}$ , influences the energy price in both MP and aCHP. It is worth noting that non-load and start-up costs do not affect the energy price.

4) *Reserve price in aCHP*: The reserve price  $\gamma_t$  is obtained by differentiating the Lagrangian dual in (17) with respect to  $\alpha_{gi,t}$ , as detailed below:

$$\begin{aligned} \gamma_t = & 2a_{gi} [M_{pt}P_{gi,t} + \alpha_{gi,t} (\sum_{pt}^2 + M_{pt}^2)] + b_{gi}M_{pt} \\ & + \mu_{i,t}^+ \hat{\delta}_{gi} + \mu_{i,t}^- \hat{\delta}_{gi} + \rho_{gi,t}^+ - \rho_{gi,t}^-. \end{aligned} \quad (19)$$

To reformulate the reserve price from the system-wide perspective, substituting (19) into (5s) yields  $\gamma_t$  as (12). Thus, in aCHP, the reserve price is not influenced by the non-load and start-up cost of the generator in the same way as MP.

5) *Inertia price in aCHP*: aCHP enables the continuous relaxation of commitment variables, ensuring that constraints (5t) are effectively bounded, in contrast to using binary variables for commitment decisions. The inertia price  $\chi_t$  is derived through the differentiation of the Lagrangian dual in (17) with respect to  $u_{gi,t}$ , as shown below:

$$\chi_t = \frac{c_{gi} + \tilde{s}_{gi,t} + \kappa_{i,t}^+ - \kappa_{i,t}^- - \rho_{gi,t}^+ - \mu_{gi,t}^+ P_{gi}^{\max} + \mu_{gi,t}^- P_{gi}^{\min}}{H_{gi} P_{gi}^{\max}}. \quad (20)$$

By substituting (20) into (8g), we obtain the inertia price as:

$$\begin{aligned} \chi_t = & \frac{\sum_{i \in \mathcal{I}} [u_{gi,t}(c_{gi} + \tilde{s}_{gi,t} - \mu_{i,t}^+ + \mu_{i,t}^- + \kappa_{i,t}^+ - \kappa_{i,t}^- - \rho_{i,t}^+)]}{P_{sys} H_{\min} - \sum_{i \in \mathcal{I}} [H_{ei,t} P_{ei}^{\max} + (H_{wi,t} + \hat{\delta}_{wi}) P_{wi}^{\max} + (H_{pi,t} + \hat{\delta}_{pi}) P_{pi}^{\max}]}. \end{aligned} \quad (21)$$

Comparing (13) and (21), the inertia price in aCHP has the distributed start-up cost  $\tilde{s}_{gi,t}$ . Hence, aCHP compensates start-up costs via inertia price, while MP cannot include the start-up cost for inertia provision.

#### D. Average incremental costs pricing

This section introduces AIP for the remuneration method inertia-aware electricity markets based on the method in [24].

1) *Average incremental costs function*: The average incremental costs, including the non-load and start-up costs for the generation output of SG, are defined as follows:

$$\begin{aligned} \hat{C}_{gi,t} = & a_{gi} [(P_{gi,t} + M_{pt}\alpha_{gi,t})^2 + \sum_{pt}^2 \alpha_{gi,t}^2] \\ & + \hat{b}_{gi} (P_{gi,t} + M_{pt}\alpha_{gi,t}), \end{aligned} \quad (22)$$

where  $\hat{b}_{gi}$  is the average cost coefficient, the non-load cost  $c_{gi}$  and the start-up cost  $s_{gi,t}$  are allocated based on the dispatched power  $\sum_{t \in [t_{on}, t_{off}]} P_{gi,t}^*$ , which is defined as:

$$\hat{b}_{gi} = b_{gi} + \frac{(\sum_{t \in [t_{on}, t_{off}]} c_{gi}) + s_{gi}}{\sum_{t \in [t_{on}, t_{off}]} P_{gi,t}^*}. \quad (23)$$

2) *Time decoupled pricing run*: By fixing the commitment set of SG from (5), the following problem is formulated to determine prices for each time period [24].

$$\min_{\Xi} \sum_{i \in \mathcal{I}} \hat{C}_{gi,t} \quad (24a)$$

$$\text{s.t.} \quad (5f), (5g), (5q) - (5t), (8b), (8c), (8g), (16), \quad (24b)$$

where  $\Xi = \{p_{gi,t}, u_{gi,t}, \alpha_{gi,t}\}$  being the set of optimization variables. Equation (24) is solved for each time interval to calculate prices by relaxing commitment variables to be continuous. As a result, the SG at the minimum generation level can set the price.

3) *Energy price in AIP*: By taking the partial derivative of the Lagrangian dual of (24) with respect to  $P_{gi,t}$ , energy price  $\lambda_{i,t}$  is derived as follows:

$$\lambda_{i,t} = 2a_{gi}(P_{gi,t} + M_{pt}\alpha_{gi,t}) + \hat{b}_{gi} + v_{gi,t}^+ - v_{gi,t}^- + \mu_{gi,t}^+ - \mu_{gi,t}^-. \quad (25)$$

The difference between (11), (18), and (25) is the average cost coefficient  $\hat{b}_{gi}$ . Thus, the energy price is affected by the average non-load and start-up costs of the marginal unit and exceeds the value in MP and aCHP.

4) *Reserve price in AIP*: The reserve price  $\gamma_t$  is obtained by differentiating the Lagrangian dual of (24) with respect to  $\alpha_{gi,t}$ , as detailed below:

$$\begin{aligned} \gamma_t = & 2a_{gi} [M_{pt} P_{gi,t} + \alpha_{gi,t} (\Sigma_{pt}^2 + M_{pt}^2)] + \hat{b}_{gi} M_{pt} \\ & + \mu_{i,t}^+ \hat{\delta}_{gi} + \mu_{gi,t}^- \hat{\delta}_{gi} + \rho_{gi,t}^+ - \rho_{gi,t}^- \end{aligned} \quad (26)$$

Thus, unlike MP and aCHP, the reserve price in AIP is also influenced by the non-load and start-up cost of the SG.

5) *Inertia price in AIP*: The inertia price  $\chi_t$  is derived by differentiating of the Lagrangian dual of (24) with respect to  $u_{gi,t}$ , and substituting into (8g), we obtain the inertia price as:

$$\begin{aligned} \chi_t = & \frac{\sum_{i \in \mathcal{I}} [u_{gi,t} (-\mu_{i,t}^+ + \mu_{i,t}^- + \kappa_{i,t}^+ - \kappa_{i,t}^- - \rho_{i,t}^+)]}{P_{sys} H_{\min} - \sum_{i \in \mathcal{I}} [H_{ei,t} P_{ei}^{\max} + (H_{wi,t} + \hat{\delta}_{wi}) P_{wi}^{\max} + (H_{pi,t} + \hat{\delta}_{pi}) P_{pi}^{\max}]} \end{aligned} \quad (27)$$

Unlike MP and aCHP, the inertia price in AIP is unaffected by non-load and start-up costs.

## V. CASE STUDIES

### A. Test Case Description

This section examines the investigated remuneration methods for inertia-aware operations using the modified IEEE 118-bus test system illustrated in Fig. 1. 28 SGs, 8 PVs, 2 WTs, and 10 ESs provide energy, reserve, and inertia. SGs are characterized by time coupling constraints such as the ramp and minimum up/down time according to [29]. RES generation profile and load are set according to historical data in Fall 2023 from CAISO [30]. The penetration of RES generation  $\eta = (20\%, 25\%, 30\%, 35\%, 40\%)$  varies for the simulation. The inertia constant of SGs is determined based on the type of generator and ranges between 3s and 10s. PV and WT provide an uniform inertia constant of 3s by deloading 5% and 10% of their maximum power output, as described by the synthetic inertia response algorithm in [28], [31]. ES can provide an inertia constant of up to 11s. Table I shows the auxiliary parameters for the simulation. All market models are implemented using the Julia JuMP package, and the code and input data are available in [32].

We set four scenarios for the numerical experiment:

- 1) Base w/o inertia: The inertia requirement constraint is not incorporated into the market model in (5). After fixing the commitment variables, the price of energy and reserve are computed as dual variables.
- 2) Base w/ inertia: SGs not dispatched in the base w/o inertia can be designated as RMR units to facilitate inertia-aware system operations. These units are manually selected based on their marginal costs in ascending order to fulfill the inertia requirements. SGs with economic losses are compensated using the uplift described in (9a). Inertia provided by IBR is settled by (9b).
- 3) MP method: Inertia-aware UC is executed according to the model presented in (5). The settlement is calculated by the prices for energy, reserve, and inertia derived through (11), (12), and (13). In addition, an uplift compensates for the economic loss of SG.

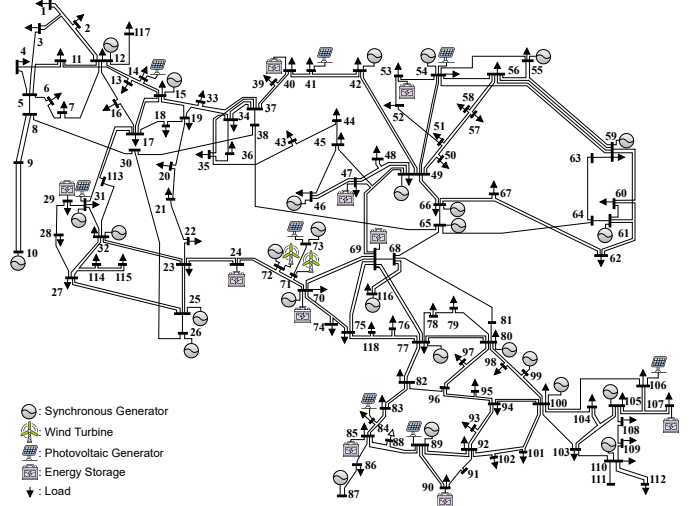


Fig. 1: Illustrating the modified 118-bus network from [33] including 28 synchronous generators, 8 photovoltaic generators, 2 wind turbines, and 10 energy storages.

- 4) aCHP method: After inertia-aware UC, The settlement is executed by the prices based on (18), (19), and (21). An uplift is also considered.
- 5) AIP method: Including an uplift, the settlement is executed using the market prices derived by (25)-(27).

### B. Inertia-aware system operation

We evaluate the effectiveness of inertia-aware operation by comparing the base w/o inertia, the base w/ inertia, the MP, and the aCHP. We use the aggregate multi-machine system frequency response model in [34] for frequency response. In this model,  $P_m$  represents the mechanical power of the turbine,  $P_e$  is the electrical power of the generator,  $P_a$  is the acceleration power, and  $\Delta f$  is the frequency deviation in Hz. The parameters are set as follows:  $F_H = 0.3$  (fraction of the total power generation by the turbine),  $T_R = 8.0$  (reheat time constant in seconds),  $D = 1.0$  (damping constant) and  $K_m = 0.95$  (mechanical power gain). Using this model, we analyze the frequency response to the outage of the largest generator ( $P^{\max} = 1,500$  MW) under each scenario at two critical times: 01:00, when system inertia is the lowest, and 08:00 when inertia meet the requirement.

1) *System inertia level*: Fig. 2 shows that the base w/o inertia cannot meet the inertia requirement of 44.28 GW-s at  $\eta = 20\%$  during off-peak periods [00:00-07:00 and 21:00-24:00]. However, from 08:00 to 20:00, all cases are shown to meet the inertia requirements regardless of the presence of

TABLE I. PARAMETER SETUP FOR THE CASE STUDY

Parameter	Value
Minimum equivalent inertia requirement, $H_{\min}$	3.5s
Maximum admissible rate of change of frequency, $f'_{\max}$	0.5Hz/s
Maximum admissible frequency deviation, $\Delta f_{\max}$	0.55Hz
Variance of the distribution, $\Sigma_{pt}$	1
Reference system frequency, $f_0$	60Hz
Mean of the distribution, M	0.5
Probability of resource's power limit violations, $\epsilon$	0.05

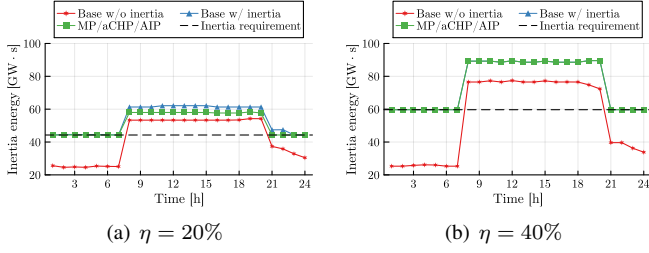


Fig. 2: Illustrating the trend of system inertia energy levels provided by all generation resources during 24-hour for each case.

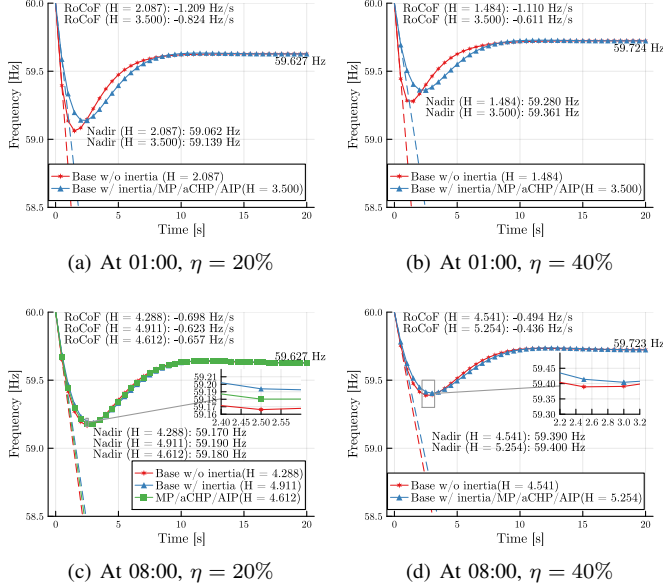


Fig. 3: Illustrating system frequency response with different inertia levels for each case.

inertia constraints. Despite increases in  $\eta$ , the trend towards inertia provision remains unchanged. All cases meet the inertia requirements of 59.68 GW·s from 08:00 to 20:00 at  $\eta = 40\%$ .

2) *Frequency stability*: Fig. 3(a) and 3(b) illustrate the system frequency response at 01:00 when inertia is the lowest during the simulation period. Regardless of  $\eta$ , the nadir is higher compared to base w/o inertia, from 59.062 Hz to 59.139 Hz and from 59.280 Hz to 59.361 Hz, representing 0.13% of improvement due to inertia-aware operation. The RoCoF is improved by approximately 50%, increasing from -1.209 Hz/s to -0.824 Hz/s and from -1.110 Hz/s to -0.611 Hz/s. However, at 08:00, Nadir and RoCoF improvements are negligible, as shown in Fig. 3(c) and 3(d). This is because the provision of inertia by SG increases as the number of committed SGs increases during the peak periods.

3) *Commitment and generation of SG* (Fig. 4): When the inertia provision by RES is fixed, and the inertia provided by ES averages only 1-2%, the base w/ inertia, the MP, the aCHP, the AIP can satisfy the inertia requirements because more SGs are committed for providing inertia compared to the base w/o inertia. In the base w/o inertia, the number of online SG units increases from 5 to 10 at 08:00 and from 4 to 11 in  $\eta = 20\%$  and  $\eta = 40\%$  in response to changes in net load as shown in Fig. 4. At 21:00, as the load decreases, the number of online

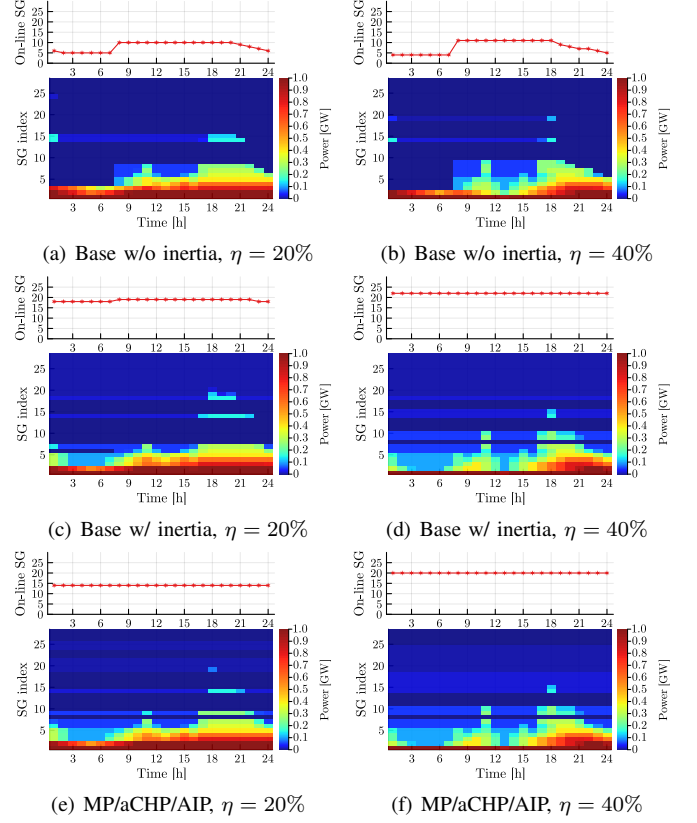


Fig. 4: Illustrating the number of online SG and the output of SG or each case (the SG index is sorted in ascending order according to marginal cost.)

SG units is reduced accordingly. In the base w/ inertia, SGs with high marginal costs (SG 16-26) not dispatched in the base w/o inertia are committed through RMR operation to meet the inertia requirements. Consequently, the number of online SG units is maintained at a minimum of 18 at  $\eta = 20\%$  and 22 at  $\eta = 40\%$ . As the SGs committed for inertia provision have high marginal costs and operate at their minimum generation limits, some mid-merit SGs (6-15 at  $\eta = 20\%$ ) are excluded from dispatch due to the need to maintain supply-demand balance and minimum generation limit. Additionally, as the number of online SGs increases compared to the base w/o inertia, the output of SGs decreases compared to the base w/o inertia. In the MP, the aCHP, and the AIP, online SG units are maintained at 14 for  $\eta = 20\%$  and 20 for  $\eta = 40\%$ . As the optimal result of the inertia-aware UC, fewer SGs are dispatched compared to the base w/ inertia while meeting the inertia requirements. For example, only SGs 19-21 and 24-26 are dispatched to provide inertia at  $\eta = 20\%$ , demonstrating more cost-effective scheduling to meet the inertia requirement.

### C. Market Prices

1) *Energy price*: Fig. 5(a) illustrates the energy prices in the MP, the aCHP, and the AIP. Although the formulation of energy price in the MP, as defined in (11), is identical to (18), the energy prices in aCHP are 8.82% higher on average compared to the MP. In the aCHP, the minimum generation limit is relaxed to 0 MW, resulting in the energy price being



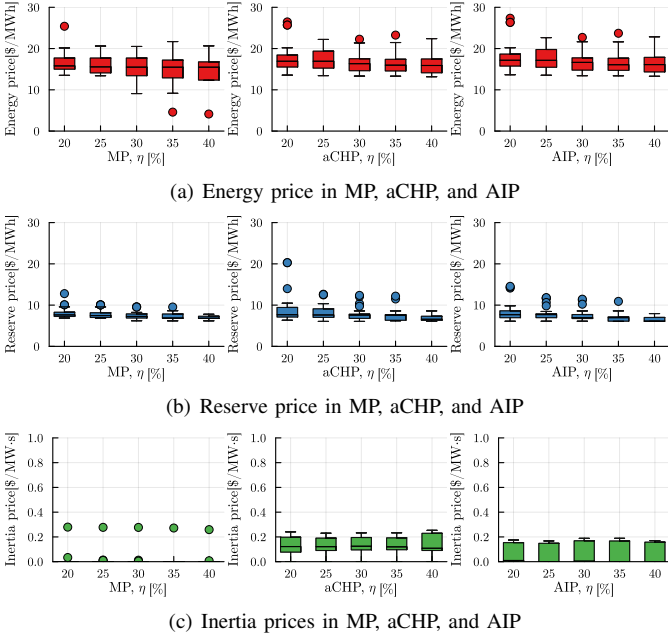


Fig. 5: Illustrating 24-hour energy, reserve, and inertia prices for each method.

determined at the minimum generation level of the marginal generator. For example, in the scenario at  $\eta = 20\%$ , SG 20 is operating under a minimum generation constraint of 20 MW at 18:00. In the MP, SG 20 cannot determine the energy price due to the minimum generation limit, resulting in the price of \$25.52/MWh, which is marginal costs of SG 19. However, In the aCHP, the energy price is determined by the marginal cost of SG 20, which is set at \$26.46/MWh at the generation level of 2.37 MW, below the minimum generation limit (20MW). The energy prices in the AIP are 1.38% higher on average than in the aCHP. According to (25), average non-load and start-up costs are added to the marginal price. For example, in the scenario at  $\eta = 20\%$ , the marginal cost of SG 20 in the AIP is \$26.65/MWh, which is the energy price.

2) *Reserve price*: The reserve price shows a pattern similar to the energy price in the MP, the aCHP, and the AIP, as shown in Fig 5(b). As  $\eta$  increases, the reserve price tends to decrease by an average of 2.5%. SGs with high marginal costs become constrained by their minimum generation limits and are subsequently excluded from determining the reserve price. However, the reserve price in the aCHP tends to increase compared to the MP because the marginal SG determining the reserve price in the aCHP is higher than the MP. For example, at 18:00, the marginal SG determining the reserve price in the MP is SG 19, while it is SG 20 in the aCHP, resulting in an increase in the reserve price at that time to \$13.99/MWh, which is \$1.29/MWh higher than the reserve price in the MP. On the other hand, according to (19) and (26), if the marginal SG supplying reserve and the value of  $\alpha_{gi,t}$  are identical in the aCHP and the AIP, the reserve price in the AIP is higher than the value in the aCHP. For example, when  $\eta$  is 20%, and SG3 provides all reserves ( $\alpha_{gi,t} = 1$ ) at 02:00, the reserve price is set at \$7.62/MWh in the aCHP and \$7.71/MWh in the AIP.

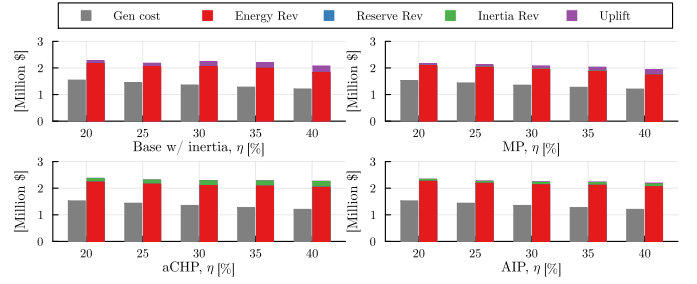


Fig. 6: Illustrating settlement results for each method regarding generation cost, energy revenue, reserve revenue, inertia revenue, and uplift.

3) *Inertia price*: The inertia price significantly differs between the MP, the aCHP, and AIP, as shown in Fig. 5(c). In the MP, the inertia price is zero on average regardless of  $\eta$ . This is because the total inertia provided by the SGs is discretely determined by the commitment variables, making the inertia requirement in (8g) non-binding. In contrast, the commitment variables are relaxed to be continuous in the aCHP. As a result, the inertia provided by the SGs is determined continuously, making the constraints of (8g) binding. In the AIP, inertia prices can have a non-zero value because the commitment variables are also relaxed to be continuous during the pricing process. However, the non-load and start-up costs are not reflected in the inertia price in the AIP. Thus, the inertia price in the AIP is lower than that in the aCHP.

#### D. Settlement results

1) *Market settlement result*: Fig. 6 illustrates the settlement results in the base w/ inertia, the MP, the aCHP, and the AIP. Among inertia-aware operation methods, base w/ inertia exhibits the highest average generation cost, reaching \$1.37 million. The total generation cost across all  $\eta$  increased by an average of 0.7% compared to the MP, the aCHP, and the AIP due to RMR operation. The average revenue received by all SGs and RESs through the market is highest in the aCHP at \$2.3 million, followed by the AIP (\$2.26 million), the base w/ inertia (\$2.19 million), and the MP (\$2.01 million). Since energy prices constitute the largest revenue share, the aCHP and the AIP yield higher revenues than other methods. Specifically, the aCHP provides more revenue than the AIP because the inertia revenue under the aCHP is, on average, more than 1.7 times higher. Meanwhile, the base w/ inertia yields more revenue than the MP due to RMR operations.

In the aCHP, uplift payments are minimal, as the market prices, including the inertia price, ensure sufficient revenue adequacy for SGs, preventing economic losses for resources. In contrast, the base w/ inertia results in an average uplift payment of \$0.13 million, covering SG compensation costs and the opportunity costs of RES inertia. Among all methods, the MP incurs the highest average uplift payment of \$0.07 million. This is due to the zero inertia price, which necessitates compensation payments to cover the economic losses of SGs.

2) *Revenue adequacy of generator*: The cost and revenue for the base generator (SG 1) in each case are presented in Fig. 7(a). SG 1 achieves revenue adequacy across all methods, as its total revenue exceeds its generation cost. In the base



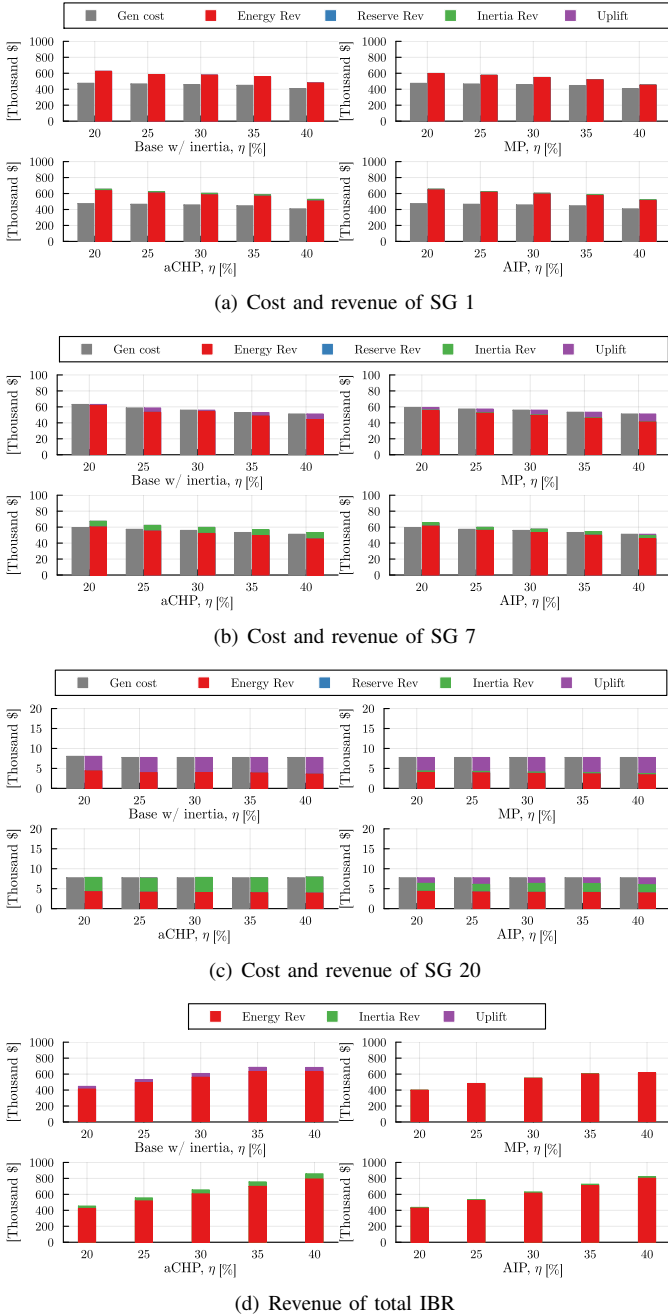


Fig. 7: Illustrating cost and revenue analysis of SG 1, SG 7, SG 20, and total renewable energy resources for each method.

w/ inertia, SG 1 is always dispatched in the market due to its low marginal cost. However, a small uplift is incurred in the base w/ inertia and the MP. As the energy price and generation output decrease, energy revenue is insufficient to ensure revenue adequacy when a start-up cost of SG 1 is incurred, necessitating an uplift. In contrast, in the aCHP and the AIP, total revenue exceeds generation costs across all  $\eta$ , obviating the need for an uplift. Thus, the aCHP and the AIP enhance profitability for the base generator.

Fig. 7(b) shows the cost and revenue of the mid-merit generator (SG 7). As  $\eta$  increases, profitability tends to decrease across all methods. SG 7 is occasionally forced to operate at its minimum generation limits because multiple SGs should be committed to provide inertia. As a result, an SG with lower

marginal costs than SG 7 determines the energy price, making it impossible to secure profitability based solely on the energy price across all scenarios. For example, the average energy price of \$16.38/MWh across all  $\eta$  in the MP, is lower than the marginal price at the minimum generation limit of SG 7, which is \$17.58/MWh. Meanwhile, an uplift is paid in the AIP. This is due to economic losses incurred from start-up costs. However, it is analyzed that the aCHP can ensure the profitability of mid-merit SGs without uplift because higher inertia prices are determined compared to the AIP.

The revenue adequacy of SG 20 is analyzed in Fig. 7(c). According to the results of the base w/ inertia, SG 20 is fully settled through uplift. Due to its high marginal costs, it is designated as an RMR unit to provide inertia. Consequently, when compensated at the energy price, it would incur economic losses, which an uplift must cover. In contrast, the MP cannot ensure revenue adequacy for SG 20. Since this unit operates only to provide inertia and thus runs at its minimum generation constraint, it cannot set the energy price. Therefore, without an uplift, \$26.04/MWh of the marginal cost at the minimum generation limit of SG 20 cannot be covered by the average energy price of \$16.38/MWh across all  $\eta$ , failing to meet revenue adequacy. In aCHP, SG 20 can secure inertia revenue due to its inertia price. This inertia revenue helps offset generation costs that cannot be covered by energy revenue alone. However, in the AIP, where the inertia price is lower, energy and inertia prices alone are insufficient to cover generation costs, necessitating an uplift.

Fig. 7(d) shows the revenue for all RES. The overall revenue increases across all cases due to the higher generation of RES. In the aCHP, RES achieves the highest average revenue of \$655,536, with an average inertia revenue of \$48,077, the highest among all cases. In the AIP, the average revenue is \$629,798, with \$15,400 attributed to inertia revenue. The revenue of RES decreases to \$530,572 in the MP compared to the base w/ inertia. Due to the zero inertia price in the MP, inertia revenue is nearly negligible, while in the base w/ inertia, inertia revenue averages \$45,969, comparable to that in the aCHP. Thus, the aCHP maximizes RES revenue, with inertia revenue similar to the deloaded energy revenue.

## VI. CONCLUSION

We renovate the inertia-aware CCUC model by incorporating time-coupling constraints for SGs and joint chance constraints to manage renewable energy uncertainty. We investigate remuneration methods for providing inertia, such as uplift, MP, aCHP, and AIP, and apply these methods to the inertia-aware operation. Simulations reveal that our model enhances the frequency stability following a contingency. Among the remuneration methods, the aCHP can ensure revenue adequacy by utilizing the inertia price and minimizing the uplift. However, the MP requires the highest level of uplift to adequately compensate generation costs, as the price function fails to account for inertia provision. The synthetic inertia compensation in the aCHP method is similar to the opportunity cost calculated from deloaded energy revenue.

## APPENDIX

## A. Deterministic Equivalent of Inertia-aware CC-UC

$$\min \sum_{t \in \mathcal{T}} \sum_{i \in \mathcal{I}} C_{gi,t} \quad (28a)$$

$$\text{s.t. } \forall t \in \mathcal{T}, \forall i \in \mathcal{I}, \forall j \in \mathcal{N}_i :$$

$$u_{gi,t}, v_{gi,t}, w_{gi,t} \in \{0, 1\}, \quad (28b)$$

$$u_{gi,t} - u_{gi,t-1} = v_{gi,t} - w_{gi,t}, \quad \forall t \in [2, T], \quad (28c)$$

$$\sum_{\tau=t-TU_{gi}+1}^t v_{gi,\tau} \leq u_{gi,t}, \quad \forall t \in [TU_{gi}, T], \quad (28d)$$

$$\sum_{\tau=t-TD_{gi}+1}^t w_{gi,\tau} \leq 1 - u_{gi,t}, \quad \forall t \in [TD_{gi}, T], \quad (28e)$$

$$-RD_{gi} \leq p_{gi,t} - p_{gi,t-1} \leq RU_{gi}, \quad (28f)$$

$$0 \leq \alpha_{gi,t} \leq u_{gi,t}, \quad (28g)$$

$$e_{i,t} \leq E_i^{\max} - 2H_{ei,t} \Delta f_{\max} P_{ei}^{\max} / f_0, \quad (28h)$$

$$e_{i,t} \geq E_i^{\min} + 2H_{ei,t} \Delta f_{\max} P_{ei}^{\max} / f_0, \quad (28i)$$

$$e_{i,t} = e_{i,t-1} + \mathbb{E}_{\Omega_{rt}} [P_{ci,t} k_i - P_{di,t} / k_i], \quad (28j)$$

$$0 \leq \alpha_{ci,t}, \alpha_{di,t} \leq 1, \quad (28k)$$

$$H_{ei,t} \leq H_{ei}^{\max}, \quad (28l)$$

$$\sum_{i \in \mathcal{I}} (\alpha_{gi,t} + \alpha_{di,t} - \alpha_{ci,t}) = 1, \quad (28m)$$

$$-F_{i,j}^{\max} \leq B_{i,j}(\theta_{i,t} - \theta_{j,t}) \leq F_{i,j}^{\max}, \quad (28n)$$

$$P_{gi,t} + P_{di,t} - P_{ci,t} + P_{wi,t} + P_{pi,t} - D_{i,t}$$

$$= \sum_{j \in \mathcal{N}_i} B_{i,j}(\theta_{i,t} - \theta_{j,t}),$$

$$P_{gi,t} \leq u_{gi,t} P_{gi}^{\max} - \hat{\delta}_{gi} \alpha_{gi,t}, \quad (28o)$$

$$-P_{gi,t} \leq -u_{gi,t} P_{gi}^{\min} - \hat{\delta}_{gi} \alpha_{gi,t},$$

$$P_{di,t} + 2H_{ei,t} f'_{\max} P_{ei}^{\max} / f_0 \leq P_{ei}^{\max} - \hat{\delta}_{di} \alpha_{di,t}, \quad (28p)$$

$$P_{ci,t} + 2H_{ei,t} f'_{\max} P_{ei}^{\max} / f_0 \leq P_{ci}^{\max} - \hat{\delta}_{ci} \alpha_{ci,t}, \quad (28q)$$

$$e_{i,t} = e_{i,t-1} + (P_{ci,t} + M_{pt} \alpha_{ci,t}) k_i - (P_{di,t} + M_{pt} \alpha_{di,t}) / k_i, \quad (28r)$$

$$\sum_{i \in \mathcal{I}} \left( u_{gi,t} H_{gi} P_{gi}^{\max} + H_{ei,t} P_{ei}^{\max} + (H_{pi,t} + \hat{\delta}_{hi}) P_{pi}^{\max} \right.$$

$$\left. + (H_{wi,t} + \hat{\delta}_{hi}) P_{wi}^{\max} \right) \geq P_{sys} H_{\min}, \quad (28s)$$

## REFERENCES

- [1] International Renewable Energy Agency (IRENA), "Renewables capacity statistics 2023." [Online]. Available: <https://www.irena.org/Data/View-data-by-topic/Capacity-and-Generation/Statistics-Time-Series>
- [2] Q.-C. Zhong and G. Weiss, "Synchronverters: Inverters that mimic synchronous generators," *IEEE transactions on industrial electronics*, vol. 58, no. 4, pp. 1259–1267, 2010.
- [3] H. Bevrani *et al.*, "Virtual synchronous generators: A survey and new perspectives," *International Journal of Electrical Power & Energy Systems*, vol. 54, pp. 244–254, 2014.
- [4] U. Markovic *et al.*, "Lqr-based adaptive virtual synchronous machine for power systems with high inverter penetration," *IEEE Transactions on Sustainable Energy*, vol. 10, no. 3, pp. 1501–1512, 2018.
- [5] N. I.-B. R. P. Task *et al.*, "Fast frequency response concepts and bulk power system reliability needs," *NERC*, p. 1, 2020.
- [6] R. Eriksson *et al.*, "Synthetic inertia versus fast frequency response: a definition," *IET renewable power generation*, vol. 12, no. 5, pp. 507–514, 2018.
- [7] A. Darbandsari and T. Amraee, "Under frequency load shedding for low inertia grids utilizing smart loads," *International Journal of Electrical Power & Energy Systems*, vol. 135, p. 107506, 2022.
- [8] P. Denholm *et al.*, "Inertia and the power grid: A guide without the spin," National Renewable Energy Lab.(NREL), Golden, CO (United States), Tech. Rep., 2020.
- [9] ERCOT, "Inertia: Basic concepts and impacts on the ercot grid," Electric Reliability Council of Texas, Tech. Rep., 2018.
- [10] Y.-K. Wu *et al.*, "Effect of system inertia on frequency response in power systems with renewable energy integration," in *2021 IEEE International Future Energy Electronics Conference (IFEEEC)*, IEEE, 2021, pp. 1–6.
- [11] NERC, "Essential reliability services whitepaper on sufficiency guidelines," North America Electric Reliability Corporation, Tech. Rep., 2016.
- [12] ERCOT, "Reliability must run (rnr) process," Electric Reliability Council of Texas, Tech. Rep., 2024.
- [13] EirGrid and SONI, "Operational constraints update," EirGrid, Tech. Rep., 2019.
- [14] D. Kelly, "System security market frameworks review final report-the aemc has published the final report for its system security market," Australian Energy Market Commission, Tech. Rep., 2017.
- [15] A. E. M. Operator, "Transfer limit advice south australia system strength for the national electricity market," 2018.
- [16] R. Doherty *et al.*, "Frequency control in competitive electricity market dispatch," *IEEE Transactions on Power Systems*, vol. 20, no. 3, pp. 1588–1596, 2005.
- [17] J. Hu *et al.*, "Inertia market: Mechanism design and its impact on generation mix," *Journal of Modern Power Systems and Clean Energy*, 2023.
- [18] M. Paturet *et al.*, "Stochastic unit commitment in low-inertia grids," *IEEE Transactions on Power Systems*, vol. 35, no. 5, pp. 3448–3458, 2020.
- [19] L. Badesa *et al.*, "Simultaneous scheduling of multiple frequency services in stochastic unit commitment," *IEEE Transactions on Power Systems*, vol. 34, no. 5, pp. 3858–3868, 2019.
- [20] Z. Liang *et al.*, "Inertia pricing in stochastic electricity markets," *IEEE Transactions on Power Systems*, vol. 38, no. 3, pp. 2071–2084, 2022.
- [21] M. Paturet *et al.*, "Economic valuation and pricing of inertia in inverter-dominated power systems," *arXiv preprint arXiv:2005.11029*, 2020.
- [22] D. Qiu *et al.*, "Market design for ancillary service provisions of inertia and frequency response via virtual power plants: A non-convex bi-level optimisation approach," *Applied Energy*, vol. 361, p. 122929, 2024.
- [23] Z. Lu *et al.*, "Convex-hull pricing of ancillary services for power system frequency regulation with renewables and carbon-capture-utilization-and-storage systems," *IEEE Transactions on Power Systems*, 2024.
- [24] R. O'Neill *et al.*, "Essays on average incremental cost pricing for independent system operators," 2019.
- [25] C. Wang *et al.*, "Commitment cost allocation of fast-start units for approximate extended locational marginal prices," *IEEE Transactions on Power Systems*, vol. 31, no. 6, pp. 4176–4184, 2016.
- [26] Y. Dvorkin, "A chance-constrained stochastic electricity market," *IEEE Transactions on Power Systems*, vol. 35, no. 4, pp. 2993–3003, 2019.
- [27] A. Kargarian *et al.*, "Chance-constrained system of systems based operation of power systems," *IEEE Transactions on Power systems*, vol. 31, no. 5, pp. 3404–3413, 2015.
- [28] M. Dreidy *et al.*, "Inertia response and frequency control techniques for renewable energy sources: A review," *Renewable and sustainable energy reviews*, vol. 69, pp. 144–155, 2017.
- [29] M. Carrion and J. Arroyo, "A computationally efficient mixed-integer linear formulation for the thermal unit commitment problem," *IEEE Transactions on Power Systems*, vol. 21, no. 3, pp. 1371–1378, 2006.
- [30] CAISO, "Caiso generation mix in 2023," <http://aiweb.techfak.uni-bielefeld.de/content/bworld-robot-control-software/>, 2008, [Online]; accessed 19-Aug-2024].
- [31] R. Villena-Ruiz *et al.*, "Assessment of the synthetic inertial response of an actual solar pv power plant," *International Journal of Electrical Power & Energy Systems*, vol. 157, p. 109875, 2024.
- [32] H. J. Kim and J. Kim, "Code supplement for inertia aware market operation," 2024, <https://github.com/githkim/inertiamarket.git>.
- [33] I. Peña *et al.*, "An extended ieeec 118-bus test system with high renewable penetration," *IEEE Transactions on Power Systems*, vol. 33, no. 1, pp. 281–289, 2018.
- [34] P. M. Anderson and M. Mirheydar, "A low-order system frequency response model," *IEEE transactions on power systems*, vol. 5, no. 3, pp. 720–729, 1990.